

[Mol Cancer Ther.](#) 2012 Oct;11(10):2158-68. doi: 10.1158/1535-7163.MCT-11-0965.

<http://mct.aacrjournals.org/content/11/10/2158.full.pdf+html>

Calcium channel TRPV6 as a potential therapeutic target in estrogen receptor negative breast cancer

Amelia A. Peters¹, Peter T. Simpson², Johnathon J. Bassett¹, Jane M. Lee¹, Leonard Da Silva^{2,3}, Lynne E. Reid², Sarah Song^{2,4}, Marie-Odile Parat¹, Sunil R. Lakhani^{2,3,5}, Paraic A. Kenny⁶, Sarah J. Roberts-Thomson¹, Gregory R. Monteith¹

1 The University of Queensland, School of Pharmacy, Brisbane, QLD, Australia; **2** The University of Queensland, UQ Centre for Clinical Research, Brisbane, QLD, Australia; **3** The University of Queensland, School of Medicine, Brisbane, QLD, Australia; **4** The University of Queensland, Queensland Centre for Medical Genomics, Institute for Molecular Bioscience, Brisbane, QLD, Australia; **5** Pathology Queensland: The Royal Brisbane & Women's Hospital, Brisbane, QLD, Australia; **6** Department of Developmental and Molecular Biology, Albert Einstein College of Medicine, New York, USA.

Running Title: Characterization of TRPV6 in Breast Cancer

Keywords: TRPV6, breast cancer, basal calcium, copy number, cell cycle

Financial support: This work was funded by two NHMRC project grants. P.T. Simpson is the recipient of a Fellowship from the National Breast Cancer Foundation, Australia. P.A. Kenny was supported by Susan G. Komen for the Cure.

Corresponding Author:

Prof Gregory Monteith

The University of Queensland, School of Pharmacy, Brisbane, Queensland, Australia, 4072

Phone: +61-7-334 61855

Fax: +61-7- 3346 1999

Email: gregm@uq.edu.au

Conflict of Interest: The authors have no conflicts of interest

Word count: 4,333; **Figures:** 5; **Tables:** 1

Abstract

Calcium signaling is a critical regulator of cell proliferation. Elevated expression of calcium channels and pumps is a characteristic of some cancers, including breast cancer. We show that the plasma membrane calcium channel TRPV6, which is highly selective for Ca^{2+} , is overexpressed in some breast cancer cell lines. Silencing of TRPV6 expression in a breast cancer cell line with increased endogenous TRPV6 expression lead to a reduction in basal calcium influx and cellular proliferation associated with a reduction in DNA synthesis. *TRPV6* gene amplification was identified as one mechanism of TRPV6 overexpression in a sub-set of breast cancer cell lines and breast tumor samples. Analysis of two independent microarray expression datasets from breast tumor samples showed that increased TRPV6 expression is a feature of estrogen receptor negative breast tumors encompassing the basal-like molecular subtype, as well as HER2-positive tumors. Breast cancer patients with high TRPV6 levels had decreased survival compared to patients with low or intermediate TRPV6 expression. Our findings suggest that inhibitors of TRPV6 may offer a novel therapeutic strategy for the treatment of estrogen receptor-negative breast cancers.

Introduction

Calcium homeostasis is tightly controlled by various calcium-transporting proteins including calcium permeable ion channels (1). Increasing evidence suggests that some cancers may be associated with perturbed regulation of intracellular free Ca^{2+} via deregulation of the expression of specific calcium transporting-proteins (2, 3). Altered calcium signaling through such changes in expression may contribute to tumorigenesis via calcium-sensitive pathways such as apoptosis, migration, and proliferation (2-4). Examples of calcium channels contributing to altered calcium signaling in cancer cells include the store operated calcium channel ORAI1 and many members of the transient receptor potential (TRP) channel family (5-10).

A TRP channel family member that has particularly high selectivity for Ca^{2+} and has constitutive activity is TRPV6 (11). TRPV6 plays a critical role in calcium absorption by the intestine (12), with TRPV6 knockout mice exhibiting signs of calcium deficiency, such as decreased bone mineral density, defective intestinal calcium absorption and reduced fertility (13). Expression of TRPV6 mRNA and protein has been detected in placenta, pancreas, intestine, prostate and mammary gland (14-16). TRPV6 expression is elevated in prostate cancer compared to normal prostate and benign prostate hyperplasia and is associated with prostate cancer progression (17-19). Studies have also implicated TRPV6 as a regulator of proliferation; stable expression of TRPV6 in HEK-293 cells increases cell proliferation (20), whereas knockdown of TRPV6 in the LNCaP prostate cancer cell line decreases proliferation and induces apoptosis (21).

Few studies have assessed TRPV6 in the context of breast cancer. Zhuang et al. (15) showed increased TRPV6 protein expression in two breast cancer tissue samples compared to normal breast. More recently and consistent with findings in prostate cancer (21), knockdown of TRPV6 decreases proliferation in T-47D breast cancer cells (7). This study also identified elevated mRNA levels (2 – 15 fold) of TRPV6 in 7 of 12 breast tumor samples (7). A very recent study has demonstrated increased levels of

TRPV6 in more invasive breast cancers (22). However differences in TRPV6 have not been correlated with pathological (e.g. histological type) or molecular (e.g. estrogen receptor (ER) status or molecular subtypes) parameters or prognosis, as has recently been shown for regulators of store-operated calcium entry (9). In this study we assessed the consequences of TRPV6 siRNA-mediated down regulation on calcium homeostasis, the cell cycle and migration in breast cancer cells. We also explored *TRPV6* gene copy number as a possible mechanism of regulating TRPV6 altered expression in breast cancer cell lines and in clinical breast cancer samples. Finally, we assessed whether TRPV6 expression is correlated with a specific subtype of breast cancer and to breast cancer survival.

Materials and Methods

Cell Culture

The MDA-MB-231 and MCF-7 cell lines were obtained directly from ATCC. MDA-MB-468 (23), T47D, BT-483, ZR-75-1, SKBR-3, 184A1 and 184B5 (24) cell lines were obtained as previously described. Upon receipt of each cell line, the cells expanded and primary, secondary, tertiary and working stocks were stored in liquid nitrogen. Cell lines were cultured for less than 10 passages (5-6 weeks) and separate media was used for each cell line. Cell lines were tested 6 monthly for mycoplasma contamination using the MycoAlert Mycoplasma Detection Assay (Lonza. Inc.; most recent test was September 2011) and monitored for morphological characteristics. Where appropriate, cell lines were characterized by assessment of the levels of HER2, ER, vimentin and E-cadherin using real time RT-PCR and/or immunohistochemistry as previously described (23). For studies that assessed the effect of TRPV6 down-regulation in the T-47D breast cancer cell line the cells were maintained in Dulbecco's Modified Eagle Medium, (high glucose) (DMEM; Invitrogen) supplemented with 10% FBS (FBS; Sigma Aldrich) and 4 mM L-Glutamine (Invitrogen) at 37°C with 5% CO₂.

Real-time RT-PCR

RNA for the analysis of TRPV6 in the cohort of cell lines and to confirm knockdown was isolated as previously described (24). RNA was reverse transcribed using the Omniscript RT kit (Qiagen) followed by real-time RT-PCR using TaqMan Universal PCR Master Mix and TaqMan gene expression assays. TRPV6 was amplified using the TaqMan[®] Gene Expression Assay Hs00367960_m1. Thermal cycling was carried out using a StepOnePlus[™] Real Time PCR System (Applied Biosystems) and universal cycling conditions. The mRNA levels were normalized to 18S rRNA and are presented relative to the appropriate control (as described in the figure legend). Relative expression levels were calculated using the comparative Ct method (25, 26).

siRNA transfection

ON-TARGET^{plus} siRNA SMARTpool[®] siRNA reagents (consisting of four rationally designed siRNAs) were purchased from Dharmacon (Millennium Science, Australia). To reduce off-target effects these siRNAs have dual strand modification (27) and their design uses an algorithm to minimize seed region matches (28). General off-target effects of TRPV6 siRNA were assessed through assessment of changes in TRPV1, cyclophilin B and E-cadherin mRNA, no changes for these targets were detected in T-47D cells (data not shown). NT siRNA had no effect on cell viability compared to mock (Dharmafect 4 without siRNA) treated T-47D cells (data not shown). T-47D cells were seeded at 5×10^3 or 7.5×10^3 cells/well in 96-well plates and transfected with TRPV6 siRNA (100 nM, 25nM of each siRNA; L-003607-00-0005) or non-targeting siRNA (NT siRNA; 100 nM, 25nM of each siRNA; D-001810-10-05) using 0.1 μ L/well DharmaFECT 4 according to the manufacturer's instructions. Knockdown of TRPV6 mRNA was assessed by real-time RT-PCR 24 h post transfection.

Measurement of Intracellular-free Ca²⁺ [Ca²⁺]_i

T-47D cells were seeded at 7.5×10^3 cells/well in a 96-well CellBIND® plates (Corning®) and transfected with the appropriate siRNA as described above. After 72 h [Ca²⁺]_i was measured using the BD™ PBX Calcium Assay Kit (BD Biosciences)(29) as previously described with minor modifications (9). Briefly, cells were loaded with the Calcium Indicator and 500 μM probenecid in physical salt solution [PSS; 140 mM NaCl, 11.5 mM glucose, 10 mM HEPES, 5.9 mM KCl, 1.4 mM MgCl₂, 1.2 mM NaH₂PO₄, 5 mM NaHCO₃, 1.8 mM CaCl₂, pH 7.3] for 1 h at 37°C. Cells were incubated for 15 min at room temperature. Loading solution was replaced with PBX signal enhancer and 500 μM probenecid in PSS with nominal Ca²⁺. BAPTA (500 μM) and CaCl₂ (0.6 mM or 2 mM) were added to the cells sequentially and fluorescence was measured at 470-495 nm excitation and 515-575 nm emission using the fluorescence imaging plate reader FLIPR^{TETRA}® (Molecular Devices). Response over baseline was assessed as a relative measure of [Ca²⁺]_i (9) and rate of Ca²⁺ influx was measured between 51 s and 151 s after Ca²⁺ addition as an assessment of TRPV6-mediated Ca²⁺ influx (7, 21).

Cell number, Cell cycle and EdU incorporation

Cell number, percentage of cells in S-phase, and cell cycle distribution were assessed in T-47D cells 120 h after siRNA treatment. T-47D cells were plated at 5×10^3 cells/well in 96-well BD Falcon™ microplates (BD Biosciences) and transfected with the appropriate siRNA. After 24 h, transfection medium was replaced with serum-free DMEM for 48-72 h. Cells were then incubated with DMEM supplemented with 8% serum for 24 h or 48 h. Cells were treated with EdU (10 mmol/L) for 1 h and then fixed with 3.7% (v/v) formaldehyde in PBS, washed with 3% (w/v) BSA in PBS and permeabilized with 0.5% Triton X-100 (v/v). Cells were then incubated with the Click-iT reaction cocktail (Alexa Fluor 555; Invitrogen), followed by DAPI (400 nM). Plates were scanned with the ImageXpress® Micro (Molecular Devices) automated epifluorescent microscope. Images were acquired with 10X objective, DAPI and EdU positive cells were

detected using DAPI-5060B and Cy3-4040B filter sets, respectively. For cell number and cell cycle analysis the DAPI integrated intensity was assessed using the cell cycle application module (MetaXpress®). The percentage of EdU positive cells was calculated using the multi wavelength cell scoring application module (MetaXpress®).

Migration assay

Cell migration assays were performed using BD FluoroBlok™ 8 µm cell culture inserts for 24-well plates (BD Biosciences). T-47D cells were seeded at 7.5×10^3 cells/well in a 96-well and transfected with the appropriate siRNA. After 72 h, the cells were trypsinized and seeded into the insert in serum-free DMEM (5×10^4 cells/350 µL). DMEM media supplemented with 1% FBS was used as the chemoattractant. After 24 h cells were labeled with 4 µg/mL Calcein AM (Invitrogen) for 1 h and fluorescence was detected at 485 nm excitation and 520 nm emission using the NOVOstar fluorescent plate reader (BMG Labtech).

Gene copy number assay

TRPV6 gene copy number was assessed using a real-time TaqMan® Copy Number Assay (Applied Biosystems). Briefly, genomic DNA (gDNA) was isolated from breast cancer cell lines using the QIAamp DNA mini kit (Qiagen) and the DNA concentration was quantified using UV absorbance (A_{260}/A_{280}). A 20 µL PCR reaction was prepared according to the Applied Biosystems TaqMan® Copy Number Assays instructions using 10 ng gDNA, TaqMan® Copy Number Reference Assay RNase P and a custom TaqMan® Assay (TRPV6_cn_for, GCTTCACCATGTGCTGCATCT; TRPV6_cn_rev, GGCTCGTGCGGTTATTGG; TRPV6_cn_pr_FAM, 6-FAM-CCCCTCAAGCCCAGG). All assays were performed in quadruplicate using the StepOnePlus™ Real Time PCR System (Applied Biosystems). Data were analyzed using CopyCaller™ v1.0 software (Applied Biosystems) by performing a comparative ($\Delta\Delta C_t$) relative quantitation analysis. The ΔC_t was determined by calculating the difference between the C_t values for TRPV6 and the reference

assay, RNase P. The $\Delta\Delta\text{Ct}$ was then measured by comparing the ΔCt for TRPV6 and the control gDNA (Applied Biosystems) which was assigned diploid copy number.

Analysis of publically available microarray data

The *TRPV6* gene resides at chromosome 7: 142,279,082-142,293,599 (hg18 assembly). Two cohorts of samples with whole genome DNA copy number data from different microarray platforms were analyzed to determine whether somatic alterations in DNA copy number occur in the *TRPV6* gene region in breast tumors. The first cohort consisted of 35 invasive ductal carcinomas, of which 22 were ER-positive and 13 were ER-negative, analyzed by 4.7k BAC-microarray comparative genomic hybridization (aCGH) (30). The second cohort was derived from The Cancer Genome Atlas (TCGA) and consisted of 247 samples analyzed using the Affymetrix Genome-Wide Human SNP Array 6.0. SNP6.0 CEL files for each sample consisting of level 3 pre-processed data of segmental values were downloaded from the TCGA Data Portal (31). The data was processed in R version 2.13.0 to score DNA copy number alterations, as described by others (32). Briefly the thresholds of <-0.3 and >0.3 were assigned to call losses and gains, respectively, and the amplitude of gain at the region of the *TRPV6* gene was assessed specifically by using thresholds of >0.3 , >0.6 , >0.8 and >1.0 . To determine the status of *TRPV6* gene copy number in different subtypes of breast cancer, this cohort was stratified using clinicopathological data available from the TCGA according to histological type (invasive ductal carcinoma (IDC) or invasive lobular carcinoma (ILC)) and biomarker expression status (ER, progesterone receptor (PR), HER2) into the following groups: ILC, IDC ER+/HER2-, IDC ER+/HER2+, IDC ER-/HER2+, IDC ER-/PR-/HER2-. This cohort was also stratified according to molecular subtype based on the gene expression profiling data from the same samples and using the Single Sample Predictor defined by Hu et al. (33).

To assess the gene expression patterns of TRPV6 in breast cancer, data were downloaded for the following two studies, the TCGA (see above) and the NKI-295 dataset (34). For the TCGA data, level 2

(log₂ lowess normalized) gene expression data for 371 tumors was downloaded from the data portal. In the NKI-295 dataset, the *TRPV6* gene was annotated under a previous name, *ABP/ZF*. The samples were stratified, as described above, using clinicopathological data according to ER status, molecular subtype and histological type plus ER/PR/HER2 biomarker expression (TCGA data only).

Statistical analysis

Statistical significance was assessed as described in individual figure legends. Data analysis was performed using Prism version 5.02 for Windows (GraphPad Inc).

Results

TRPV6 is overexpressed in a subset of breast cancer cell lines

Increased TRPV6 levels are a feature of T-47D breast cancer cells compared to MDA-MB-231 and MCF-7 breast cancer cells (35). TRPV6 expression is also elevated (2-15 fold) in 7 of 12 clinical breast tumors (7). To begin to assess if TRPV6 overexpression may be a feature of specific breast cancer subtypes we assessed TRPV6 levels in a bank of non-malignant and malignant breast cancer cell lines varying in ER, PR and HER2 status and molecular subtype. TRPV6 levels were elevated in 4 cell lines; ZR-75-1, T-47D, SK-BR-3 and MDA-MB-468 compared to the non-malignant breast cancer cell lines 184A1 and 184B5 (Fig. 1A). Levels in these four breast cancer cell lines were greater than 60 fold higher relative to 184A1 cells (Fig. 1A), whereas TRPV6 levels in MDA-MB-231, MCF-7 and BT-483 were similar (< 7 fold higher to those observed in 184A1 cells) (Fig. 1A).

Knockdown of TRPV6 reduces the rate of calcium influx

TRPV6 basal Ca^{2+} influx has previously been assessed as a measure of TRPV6 function in HEK293 cells transiently overexpressing TRPV6 (36), in LNCaP prostate cancer cells (21) and in T-47D breast cancer cells, where a functional consequence of TRPV6 siRNA was shown by the addition of supra-physiological levels of extracellular Ca^{2+} (10 mM) (7). Here we investigated the effect of TRPV6 knockdown via siRNA (Fig. 1B) on the function of the TRPV6 channel basal calcium influx in T-47D breast cancer cells. We observed a basal Ca^{2+} influx reduced by 44% after the addition of either 0.6 mM or 2 mM extracellular calcium in cells with TRPV6 targeted knockdown compared to cells with non-targeting control (Fig. 1C and 1D). These results demonstrate functional alterations in calcium homeostasis associated with TRPV6 knockdown in T-47D breast cancer cells at physiological concentrations of extracellular Ca^{2+} re-addition.

Effect of TRPV6 knockdown on viable cell number, cell cycle, and migration

We investigated potential effect of TRPV6 down-regulation (Fig. 2A) on the cell cycle and cell migration in T-47D breast cancer cells. TRPV6 siRNA significantly reduced the number of viable cells at 24 h and 48 h (35% and 40% reduction, respectively) in the presence of serum (Fig. 2B). Assessment of proliferating cells using EdU staining, showed that the percentage of cells in S-phase significantly decreased (~20%) with TRPV6 knockdown (Fig. 2C). DNA-content histogram analysis showed that TRPV6 knockdown caused cells to accumulate in the G1-phase at 24 h with serum (Fig. 2D), but not at 48 h with serum (Fig. 2E). Knockdown of TRPV6 did not decrease T-47D migration; instead a modest increase was observed (Fig. 2F).

TRPV6 gene amplification in a bank of breast cancer cell lines

To assess whether gene amplification could be a mechanism for TRPV6 mRNA overexpression in some breast cancer cell lines, gene copy number was assessed using a real-time assay. TRPV6 copy number was greater than 6 in T-47D, SK-BR-3, ZR-75-1, BT-483 and MCF-7 cells (Fig. 3A). The highest level was detected in BT-483 cells (9 copies) (Fig. 3A). Overexpression of TRPV6 mRNA in ZR-75-1, T-47D and SK-

BR-3 cells may be due, at least in part, to increased gene copy number (Fig. 3B). However, an association between gene copy number and mRNA levels for TRPV6 was not observed for MDA-MB-231, MCF-7, BT-483 or MDA-MB-468 cells (Fig. 3B).

TRPV6 gene amplification in clinical breast tumors

To ascertain if *TRPV6* gene is subjected to copy number alteration in human breast tumor samples, *TRPV6* gene copy number was examined in data from two cohorts of invasive carcinomas derived from BAC aCGH (cohort 1) (30) and SNP-CGH (TCGA – cohort 2) platforms. The genomic region harboring the *TRPV6* gene was subjected to both gains and deletions. The frequency of these gains and deletions differed across different tumor subtypes (Table 1). For instance, both cohorts demonstrated a significant increase in the frequency of *TRPV6* gene copy number gains in ER-negative tumors relative to ER-positive tumors ($P < 0.01$). This finding was also observed when triple negative tumors (ER-, PR-, and HER2-negative) were compared to ER-positive or HER2-positive tumors and when basal-like tumors were compared to luminal A or HER2 tumor types ($P < 0.01$; Table 1).

The amplitude of gain was further measured using different thresholds for calling gains to determine the number of tumors with higher level gains (amplifications) in the region of *TRPV6* (Fig. 4A and 4B) and determine, according to the copy number profile, whether there was a specific amplification in this region or whether the region was gained as part of an increase copy number covering a large region of the chromosome. Figure 4A shows a peak in gains very close to, but not encompassing the *TRPV6* gene locus, highlighted by the red line. We identified 6 tumors overall (4 from cohort 1 and 2 from cohort 2) that had specific amplification in the region of the *TRPV6* gene (Fig. 4A and 4B), the increase in copy number for the remaining samples were reflected by increased DNA copy number of chromosome 7q not specifically related to *TRPV6* gene region. The gene region was lost most frequently in HER2 tumors when compared to ER-positive or triple negative tumors and in comparison to basal-like tumors ($P <$

0.01; Table 1). The correlation between *TRPV6* gene copy number and TRPV6 mRNA levels was strongest for the basal-like subtype compared to other molecular subtypes (Fig. 4C).

***TRPV6* gene expression in clinical breast tumors and association with survival**

Given the evidence from the current study and others, that TRPV6 overexpression is a feature of some specific breast cancers, we evaluated published transcription profiling data from two independent cohorts of invasive breast tumors, the NKI-295 dataset comprising 295 primary tumors (34) and TCGA comprising 372 tumors. The gene expression levels were assessed in tumors stratified according to ER status, molecular subtype and immunophenotype. These results showed that TRPV6 mRNA levels are increased in ER-negative tumors compared to ER-positive tumors (Fig. 5A and 5B). When the tumors in the cohort were assigned to molecular subtypes based on the gene expression profiles, TRPV6 expression was significantly elevated in basal-like and HER2 breast tumors compared to luminal A and luminal B breast tumors (Fig. 5C and 5D). Additionally, when stratified by immunophenotype, TRPV6 expression was elevated in HER2-positive and triple negative ductal tumors compared to ER-positive, HER2-negative tumors (Fig. 5E). Finally, when the tumors were stratified according the level of TRPV6 mRNA expression, tumors with the highest levels of expression (upper quartile) were associated with a significantly reduced overall survival when compared to tumors in the intermediate or lower quartiles (Fig. 5F).

Discussion

TRPV6 is an essential calcium influx channel, which has been implicated in prostate cancer progression (18, 19). Elevated TRPV6 expression is seen in breast tumors (7), however, the mechanism of overexpression has not been addressed and a correlation with tumor subtype or prognosis also not determined. Our studies identify *TRPV6* gene amplification as a possible mechanism for TRPV6 overexpression in some breast tumors. We provide further evidence for a role for TRPV6 in tumor

progression with siRNA-mediated inhibition of TRPV6 reducing basal Ca^{2+} influx and breast cancer cell proliferation. Increased TRPV6 expression was a feature of ER-negative, HER2 and basal-like breast tumors and increased TRPV6 levels were associated with reduced survival in breast cancer patients.

Elevated TRPV6 mRNA levels have previously been observed in seven of 12 clinical breast cancer samples and in the T-47D breast cancer cell line compared to the MDA-MB-231 and MCF-7 cell lines (7). Elevated TRPV6 was identified in four of seven breast cancer cell lines assessed in this study with no obvious correlation between TRPV6 expression levels and molecular subtype but this may simply be due to the small number of cell lines examined. Analysis of two independent cohorts of clinical samples, however, identified a correlation between TRPV6 mRNA expression levels and i) immunophenotype and ii) molecular subtypes. These data highlight a potential biological role for TRPV6 in specific breast cancer subtypes. For instance the highest TRPV6 mRNA levels were consistently associated with invasive ductal carcinomas with an ER-negative phenotype, whether they were classified simply as ER-negative, as triple negative (ER-, PR- and HER2-negative) or as basal-like (gene expression profiling subtype). The correlation we observed between elevated TRPV6 expression and a significantly decreased survival may reflect the association between TRPV6 expression and the ER-negative subgroup, which are among those breast cancers with the worst prognosis (37, 38).

Genome-wide, high resolution studies of breast cancer samples show that between 10.5 - 12% of overexpressed genes are associated with gene amplification (39, 40). We explored whether increased gene copy number was a potential driver of enhanced expression levels seen in some breast cancers. We found an association between increased TRPV6 mRNA expression and increased *TRPV6* gene copy number in three breast cancer cell lines, ZR-75-1, T-47D and SK-BR-3. Analysis of clinical breast cancer samples showed that although *TRPV6* gene does not reside within a region of the genome that is frequently amplified in breast cancer (such as, 8p12, 8q24, 11q13, 17q12 (41)), the gene was subjected

to frequent somatic alteration and that elevated copy number was most likely to occur in ER-negative, triple negative or basal-like compared to other subtypes.

We tested whether there was a correlation between *TRPV6* gene expression levels and gene copy number data in the TCGA cohort of clinical samples, where both data were available. The highest correlation was found in the basal-like subgroup where a proportion of tumors exhibited both an elevated DNA copy number and an increased mRNA level. The data suggest gene amplification as a possible mechanism for driving TRPV6 overexpression in these cell lines and tumors. In contrast, TRPV6 expression did not correlate with gene copy number in four breast cancer cell lines and in many tumors, suggesting that there is an alternative mechanism driving the high levels of gene transcription. This scenario is not unexpected in breast cancer, since mRNA levels are not always linearly related to gene copy number and where numerous alternative mechanisms for regulating transcription exist, including altered miRNA regulation, DNA methylation or transcriptional activation (42). Solvang et al. (42) showed that a quadratic relationship for copy number and mRNA expression was a better fit than a linear relationship for more than 80% of the breast tumors assessed. Furthermore a gene may exhibit two expression sub-sets in a breast cancer cohort; such as amplification without a corresponding increase in expression and increased expression without amplification (42). Such a scenario may exist for TRPV6 in breast cancer cell lines and tumors.

The functional role for TRPV6 was investigated in the T-47D breast cancer cell line, which has elevated TRPV6 mRNA expression and gene copy number. Knockdown of TRPV6 using siRNA significantly decreased basal Ca^{2+} influx with the addition of physiological levels of Ca^{2+} , consistent with the one previous study of TRPV6 activity in a breast cancer cell line (7). Our current findings and those of Bolanz et al. (7) also identify a reduction in viable cell number with TRPV6 siRNA treatment in T-47D cells. While Bolanz et al. (7) suggested an increase in the number of cells undergoing apoptosis our data also suggest

that TRPV6 siRNA reduces the percentage of cells in S-phase and increases the percentage of cells in the G1-phase. Ca^{2+} influx is a well known mechanism to promote the G1 to S-phase transition (43), therefore the accumulation of cells in G1-phase is likely to be associated with the attenuation of calcium influx associated with TRPV6 inhibition. LNCaP prostate cancer cells also have a reduction in cells in S-phase, but no affect on the percentage of cells in the G1-phase with TRPV6 knockdown (21). This indicates some potential divergent roles for TRPV6 on cell cycle in breast and prostate cancer cells. Although, TRPV6 down-regulation decreases breast cancer cell proliferation, knockdown of TRPV6 expression actually increased T-47D breast cancer cell migration, even though viable cell number was reduced. This may suggest that the influence TRPV6 has on outcome or prognosis is via mechanisms other than tumor cell migration. However, this is in contrast to a very recent study in MDA-MB-231 and MCF-7 breast cancer cell lines, where TRPV6 silencing reduced migration (22). Further studies assessing the role of TRPV6 in the migration of other breast cancer cell lines are now required.

The potential requirement for TRPV6 function specifically in tumor cell proliferation, through calcium influx, may highlight the underlying association between elevated TRPV6, an ER-negative tumor phenotype and poor outcome, since ER-negative tumors are most often of high grade and are highly proliferative tumors. It is unclear from this study whether TRPV6 overexpression drives or simply facilitates this enhanced proliferation in this aggressive breast tumor subtype. Nevertheless, targeted knockdown of the gene in cells with elevated expression leads to reduced growth and stalling of the cell cycle suggesting that targeting the TRPV6 calcium channel maybe a useful therapeutic mechanism.

There is a requirement for targeted therapeutics in ER-negative, non-HER2 positive tumors owing to the lack of clinical benefit derived from giving these patients current targeted therapy (44) (Herceptin® or endocrine-based treatment). Chemotherapeutics such as taxanes do provide clinical benefit and the use of poly(ADP-ribose) polymerase inhibitors (PARPi) show promise by targeting apparent defects in DNA

repair mechanisms in this category of breast tumors (45, 46). Much still needs to be resolved regarding the role of PARPi in treating ER-negative tumors and recent phase III clinical data for PARPi are somewhat disappointing (47) indicating that alternative therapeutic options, such as targeting calcium signaling are warranted.

Inhibition of the calcium channel TRPV6 may not be associated with the predicted systemic side effects that would result from inhibition of some other calcium channels, since TRPV6 knockout mice are viable and exhibit traits that may be well tolerated compared to current therapies (e.g. decreased bone mineral density and defective intestinal calcium absorption (13)). Our studies indicate that TRPV6 inhibitors are potential therapeutics for the treatment of ER-negative breast cancers that exhibit elevated TRPV6 expression.

Acknowledgements

The authors would like to acknowledge the contribution of tissues donors and research groups to the generation of The Cancer Genome Atlas (TCGA) data resource.

Grant support

This work was funded by a NHMRC project grant (569645) awarded to G.R. Monteith, S.J. Roberts-Thomson, P.T. Simpson and M.O. Parat and an NHMRC Project grant (631347) awarded to G.R.

Monteith, S.J. Roberts-Thomson and J. W. Holland. P.T. Simpson is the recipient of a Fellowship from the National Breast Cancer Foundation, Australia. P.A. Kenny was supported by Susan G. Komen (KG100888).

References

1. Berridge MJ, Bootman MD, Roderick HL. Calcium signalling: dynamics, homeostasis and remodelling. *Nat Rev Mol Cell Biol.* 2003;4:517-29.
2. Monteith GR, McAndrew D, Faddy HM, Roberts-Thomson SJ. Calcium and cancer: targeting Ca²⁺ transport. *Nat Rev Cancer.* 2007;7:519-30.
3. Roderick HL, Cook SJ. Ca²⁺ signalling checkpoints in cancer: remodelling Ca²⁺ for cancer cell proliferation and survival. *Nat Rev Cancer.* 2008;8:361-75.
4. Prevarskaya N, Skryma R, Shuba Y. Calcium in tumour metastasis: new roles for known actors. *Nat Rev Cancer.* 2011;11:609-18.
5. Yang SL, Cao Q, Zhou KC, Feng YJ, Wang YZ. Transient receptor potential channel C3 contributes to the progression of human ovarian cancer. *Oncogene.* 2009;28:1320-8.
6. Bode AM, Cho YY, Zheng D, Zhu F, Ericson ME, Ma WY, et al. Transient receptor potential type vanilloid 1 suppresses skin carcinogenesis. *Cancer Res.* 2009;69:905-13.
7. Bolanz KA, Hediger MA, Landowski CP. The role of TRPV6 in breast carcinogenesis. *Mol Cancer Ther.* 2008;7:271-9.
8. Roberts-Thomson SJ, Peters AA, Grice DM, Monteith GR. ORAI-mediated calcium entry: mechanism and roles, diseases and pharmacology. *Pharmacol Ther.* 2010;127:121-30.
9. McAndrew D, Grice DM, Peters AA, Davis FM, Stewart T, Rice M, et al. ORAI1-mediated calcium influx in lactation and in breast cancer. *Mol Cancer Ther.* 2011;10:448-60.
10. Prevarskaya N, Zhang L, Barritt G. TRP channels in cancer. *Biochim Biophys Acta.* 2007;1772:937-46.
11. den Dekker E, Hoenderop JG, Nilius B, Bindels RJ. The epithelial calcium channels, TRPV5 & TRPV6: from identification towards regulation. *Cell Calcium.* 2003;33:497-507.

12. van Abel M, Hoenderop JG, Bindels RJ. The epithelial calcium channels TRPV5 and TRPV6: regulation and implications for disease. *Naunyn Schmiedebergs Arch Pharmacol.* 2005;371:295-306.
13. Bianco SD, Peng JB, Takanaga H, Suzuki Y, Crescenzi A, Kos CH, et al. Marked disturbance of calcium homeostasis in mice with targeted disruption of the *Trpv6* calcium channel gene. *J Bone Miner Res.* 2007;22:274-85.
14. Peng JB, Chen XZ, Berger UV, Weremowicz S, Morton CC, Vassilev PM, et al. Human calcium transport protein CaT1. *Biochemical and Biophysical Research Communications.* 2000;278:326-32.
15. Zhuang L, Peng JB, Tou L, Takanaga H, Adam RM, Hediger MA, et al. Calcium-selective ion channel, CaT1, is apically localized in gastrointestinal tract epithelia and is aberrantly expressed in human malignancies. *Lab Invest.* 2002;82:1755-64.
16. Hoenderop JG, Vennekens R, Muller D, Prenen J, Droogmans G, Bindels RJ, et al. Function and expression of the epithelial Ca(2+) channel family: comparison of mammalian ECaC1 and 2. *J Physiol.* 2001;537:747-61.
17. Wissenbach U, Niemeyer BA, Fixemer T, Schneidewind A, Trost C, Cavalie A, et al. Expression of CaT-like, a novel calcium-selective channel, correlates with the malignancy of prostate cancer. *J Biol Chem.* 2001;276:19461-8.
18. Peng JB, Zhuang L, Berger UV, Adam RM, Williams BJ, Brown EM, et al. CaT1 expression correlates with tumor grade in prostate cancer. *Biochem Biophys Res Commun.* 2001;282:729-34.
19. Fixemer T, Wissenbach U, Flockerzi V, Bonkhoff H. Expression of the Ca²⁺-selective cation channel TRPV6 in human prostate cancer: a novel prognostic marker for tumor progression. *Oncogene.* 2003;22:7858-61.

20. Schwarz EC, Wissenbach U, Niemeyer BA, Strauss B, Philipp SE, Flockerzi V, et al. TRPV6 potentiates calcium-dependent cell proliferation. *Cell Calcium*. 2006;39:163-73.
21. Lehen'kyi V, Flourakis M, Skryma R, Prevarskaya N. TRPV6 channel controls prostate cancer cell proliferation via Ca(2+)/NFAT-dependent pathways. *Oncogene*. 2007;26:7380-5.
22. Dhennin-Duthille I, Gautier M, Faouzi M, Guilbert A, Brevet M, Vaudry D, et al. High expression of transient receptor potential channels in human breast cancer epithelial cells and tissues: correlation with pathological parameters. *Cell Physiol Biochem*. 2011;28:813-22.
23. Davis FM, Kenny PA, Soo ET, van Denderen BJ, Thompson EW, Cabot PJ, et al. Remodeling of Purinergic Receptor-Mediated Ca Signaling as a Consequence of EGF-Induced Epithelial-Mesenchymal Transition in Breast Cancer Cells. *PLoS One*. 2011;6:e23464.
24. Lee WJ, Roberts-Thomson SJ, Monteith GR. Plasma membrane calcium-ATPase 2 and 4 in human breast cancer cell lines. *Biochem Biophys Res Commun*. 2005;337:779-83.
25. Aung CS, Ye W, Plowman G, Peters AA, Monteith GR, Roberts-Thomson SJ. Plasma membrane calcium ATPase 4 and the remodeling of calcium homeostasis in human colon cancer cells. *Carcinogenesis*. 2009;30:1962-9.
26. Suchanek KM, May FJ, Robinson JA, Lee WJ, Holman NA, Monteith GR, et al. Peroxisome proliferator-activated receptor alpha in the human breast cancer cell lines MCF-7 and MDA-MB-231. *Mol Carcinog*. 2002;34:165-71.
27. Jackson AL, Burchard J, Leake D, Reynolds A, Schelter J, Guo J, et al. Position-specific chemical modification of siRNAs reduces "off-target" transcript silencing. *RNA*. 2006;12:1197-205.
28. Birmingham A, Anderson EM, Reynolds A, Ilesley-Tyree D, Leake D, Fedorov Y, et al. 3' UTR seed matches, but not overall identity, are associated with RNAi off-targets. *Nat Methods*. 2006;3:199-204.

29. Liu K, Titus S, Southall N, Zhu P, Inglese J, Austin CP, et al. Comparison on functional assays for Gq-coupled GPCRs by measuring inositol monophosphate-1 and intracellular calcium in 1536-well plate format. *Current chemical genomics*. 2008;1:70-8.
30. Pierga JY, Reis-Filho JS, Cleator SJ, Dexter T, Mackay A, Simpson P, et al. Microarray-based comparative genomic hybridisation of breast cancer patients receiving neoadjuvant chemotherapy. *Br J Cancer*. 2007;96:341-51.
31. The Cancer Genome Atlas (TCGA) Data Portal [Internet] Bethesda: The Cancer Genome Atlas Program National Cancer Institute at NIH; [cited 2011 April 15]. Available from: <https://tcga-data.nci.nih.gov/tcga/>.
32. Gorringer KL, George J, Anglesio MS, Ramakrishna M, Etemadmoghadam D, Cowin P, et al. Copy number analysis identifies novel interactions between genomic loci in ovarian cancer. *PLoS One*. 2010;5.
33. Hu Z, Fan C, Oh DS, Marron JS, He X, Qaqish BF, et al. The molecular portraits of breast tumors are conserved across microarray platforms. *BMC Genomics*. 2006;7:96.
34. van de Vijver MJ, He YD, van't Veer LJ, Dai H, Hart AA, Voskuil DW, et al. A gene-expression signature as a predictor of survival in breast cancer. *N Engl J Med*. 2002;347:1999-2009.
35. Bolanz KA, Kovacs GG, Landowski CP, Hediger MA. Tamoxifen inhibits TRPV6 activity via estrogen receptor-independent pathways in TRPV6-expressing MCF-7 breast cancer cells. *Mol Cancer Res*. 2009;7:2000-10.
36. Kovacs G, Danko T, Bergeron MJ, Balazs B, Suzuki Y, Zsembery A, et al. Heavy metal cations permeate the TRPV6 epithelial cation channel. *Cell Calcium*. 2011;49:43-55.
37. Sorlie T, Tibshirani R, Parker J, Hastie T, Marron JS, Nobel A, et al. Repeated observation of breast tumor subtypes in independent gene expression data sets. *Proc Natl Acad Sci U S A*. 2003;100:8418-23.

38. Bentzon N, Durning M, Rasmussen BB, Mouridsen H, Kroman N. Prognostic effect of estrogen receptor status across age in primary breast cancer. *Int J Cancer*. 2008;122:1089-94.
39. Pollack JR, Sorlie T, Perou CM, Rees CA, Jeffrey SS, Lonning PE, et al. Microarray analysis reveals a major direct role of DNA copy number alteration in the transcriptional program of human breast tumors. *Proc Natl Acad Sci U S A*. 2002;99:12963-8.
40. Hyman E, Kauraniemi P, Hautaniemi S, Wolf M, Mousses S, Rozenblum E, et al. Impact of DNA amplification on gene expression patterns in breast cancer. *Cancer Res*. 2002;62:6240-5.
41. Cuny M, Kramar A, Courjal F, Johannsdottir V, Iacopetta B, Fontaine H, et al. Relating genotype and phenotype in breast cancer: an analysis of the prognostic significance of amplification at eight different genes or loci and of p53 mutations. *Cancer Res*. 2000;60:1077-83.
42. Solvang HK, Lingjaerde OC, Frigessi A, Borresen-Dale AL, Kristensen VN. Linear and non-linear dependencies between copy number aberrations and mRNA expression reveal distinct molecular pathways in breast cancer. *BMC Bioinformatics*. 2011;12:197.
43. Santella L, Ercolano E, Nusco GA. The cell cycle: a new entry in the field of Ca²⁺ signaling. *Cell Mol Life Sci*. 2005;62:2405-13.
44. Schneider BP, Winer EP, Foulkes WD, Garber J, Perou CM, Richardson A, et al. Triple-negative breast cancer: risk factors to potential targets. *Clin Cancer Res*. 2008;14:8010-8.
45. O'Shaughnessy J, Osborne C, Pippen JE, Yoffe M, Patt D, Rocha C, et al. Iniparib plus chemotherapy in metastatic triple-negative breast cancer. *N Engl J Med*. 2011;364:205-14.
46. Tutt A, Robson M, Garber JE, Domchek SM, Audeh MW, Weitzel JN, et al. Oral poly(ADP-ribose) polymerase inhibitor olaparib in patients with BRCA1 or BRCA2 mutations and advanced breast cancer: a proof-of-concept trial. *Lancet*. 2010;376:235-44.
47. O'Shaughnessy J, Schwartzberg LS, Danso MA, Rugo HS, Miller K, Yardley DA, et al. A randomized phase III study of iniparib (BSI-201) in combination with gemcitabine/carboplatin (G/C) in

- metastatic triple-negative breast cancer (TNBC). *Journal of Clinical Oncology*. 2011;29:suppl; abstr 1007.
48. Kao J, Salari K, Bocanegra M, Choi YL, Girard L, Gandhi J, et al. Molecular profiling of breast cancer cell lines defines relevant tumor models and provides a resource for cancer gene discovery. *PLoS One*. 2009;4:e6146.
49. Neve RM, Chin K, Fridlyand J, Yeh J, Baehner FL, Fevr T, et al. A collection of breast cancer cell lines for the study of functionally distinct cancer subtypes. *Cancer Cell*. 2006;10:515-27.

Table 1: DNA copy number status of *TRPV6* gene region in breast cancer subtypes

| Cohort 1 | Total | Gains | No Gains | p-value | Losses | No Losses | p-value |
|----------------------------|--------------|--------------|-----------------|---------------------|---------------|------------------|----------------------|
| IDC | 35 | 12 (34%) | 23 (66%) | | 6 (17%) | 29 (83%) | |
| IDC ER+ | 22 | 3 (14%) | 19 (86%) | | 5 (23%) | 17 (77%) | |
| IDC ER- | 13 | 9 (69%) | 4 (31%) | 0.0022 ¹ | 1 (8%) | 12 (92%) | |
| Cohort 2 | Total | Gains | No Gains | p-value | Losses | No Losses | p-value |
| IDC | 206 | 23 (11.2%) | 183 (88.8%) | | 24 (11.6%) | 182 (88.4%) | |
| ILC | 23 | 2 (8.7%) | 21 (91.3%) | | 4 (17.4%) | 19 (82.6%) | |
| IDC ER+ | 167 | 12 (7.2%) | 155 (92.8%) | | 22 (13.2%) | 145 (86.8%) | |
| IDC ER- | 39 | 11 (28.2%) | 28 (71.8%) | 0.0007 ² | 2 (5.1%) | 37 (94.9%) | |
| IDC (ER+/HER2-) | 145 | 11 (9.1%) | 134 (90.0%) | 0.0002 ³ | 14 (9.7%) | 131 (90.3%) | 0.0060 ⁵ |
| IDC (HER2+) | 30 | 1 (4.5%) | 29 (95.5%) | 0.0026 ⁴ | 9 (30%) | 21 (70%) | |
| IDC (ER-/PR-/HER2-) | 31 | 11 (35.4%) | 20 (64.6%) | | 1 (3.2%) | 30 (96.8%) | 0.0057 ⁶ |
| Molecular Subtype | 247 | 25 (10.1%) | 222 (89.9%) | | 31 (13.0%) | 215 (87.0%) | |
| Luminal A | 93 | 5 (5.4%) | 88 (94.6%) | 0.0031 ⁷ | 11 (11.8%) | 82 (88.2%) | |
| Luminal B | 60 | 6 (10%) | 54 (90%) | | 10 (16.7%) | 50 (83.3%) | 0.0319 ⁹ |
| HER2 | 40 | 2 (5%) | 38 (95%) | 0.0219 ⁸ | 9 (22.5%) | 31 (77.5%) | |
| Basal-like | 54 | 12 (22.2%) | 42 (77.8%) | | 2 (3.7%) | 52 (96.3%) | 0.0078 ¹⁰ |

+: positive; -: negative; IDC: invasive ductal carcinoma; ILC: invasive lobular carcinoma; ER: estrogen receptor; PR: progesterone receptor.

Statistical analysis was performed using Fisher's exact test, two tailed, and only significant (< 0.05) *P*-values are displayed.

¹: cohort 1 IDC ER+ vs. ER-; ²: cohort 2 IDC ER+ vs. ER-; ³: IDC (ER-/PR-/HER-) vs. IDC (ER+/HER2-); ⁴: IDC (ER-/PR-/HER-) vs. IDC (HER2+); ⁵: IDC (HER2+) vs. IDC (ER+/HER2-); ⁶: IDC (HER2+) vs. IDC (ER-/PR-/HER-); ⁷: Basal-like vs. luminal A; ⁸: Basal-like vs. HER2; ⁹: luminal B vs. Basal-like; ¹⁰: HER2 vs. Basal-like.

Figure legends

Figure 1: Characterization of TRPV6 in breast cell lines. A, TRPV6 mRNA levels in non-malignant 184A1 and 184B5 and malignant MDA-MB-231, MCF-7, BT-483, ZR-75-1, T-47D, SK-BR-3 and MDA-MB-468 breast cell lines. Molecular features of these lines (according to (48, 49)) is given: ER, estrogen receptor; PR, progesterone receptor; Bb, Basal B; Ba, Basal A; L, Luminal. Data represent the mean \pm SD ($N = 3$) and are representative of two independent assays. B, Relative TRPV6 mRNA levels in T-47D breast cancer cells 24 h after treatment with non-targeting siRNA (NT siRNA) or TRPV6 siRNA. The data are mean \pm SD ($N = 4$) and are from two independent experiments and * $P < 0.001$ compared with NT siRNA using an unpaired t-test. C and D, effect of TRPV6 down-regulation on basal Ca^{2+} influx. C, relative $[\text{Ca}^{2+}]_i$ as mean fluorescence relative to baseline ($N = 3$). Cells were treated with 2 mM (solid line) or 0.6 mM Ca^{2+} (dotted line). Data are representative of three independent assays carried out in triplicate. D, rate of Ca^{2+} influx between 51s and 151s after Ca^{2+} addition. Data are from three independent assays carried out in triplicate (mean \pm SD; $N = 9$) and * $P < 0.001$ compared with NT siRNA using an unpaired t-test.

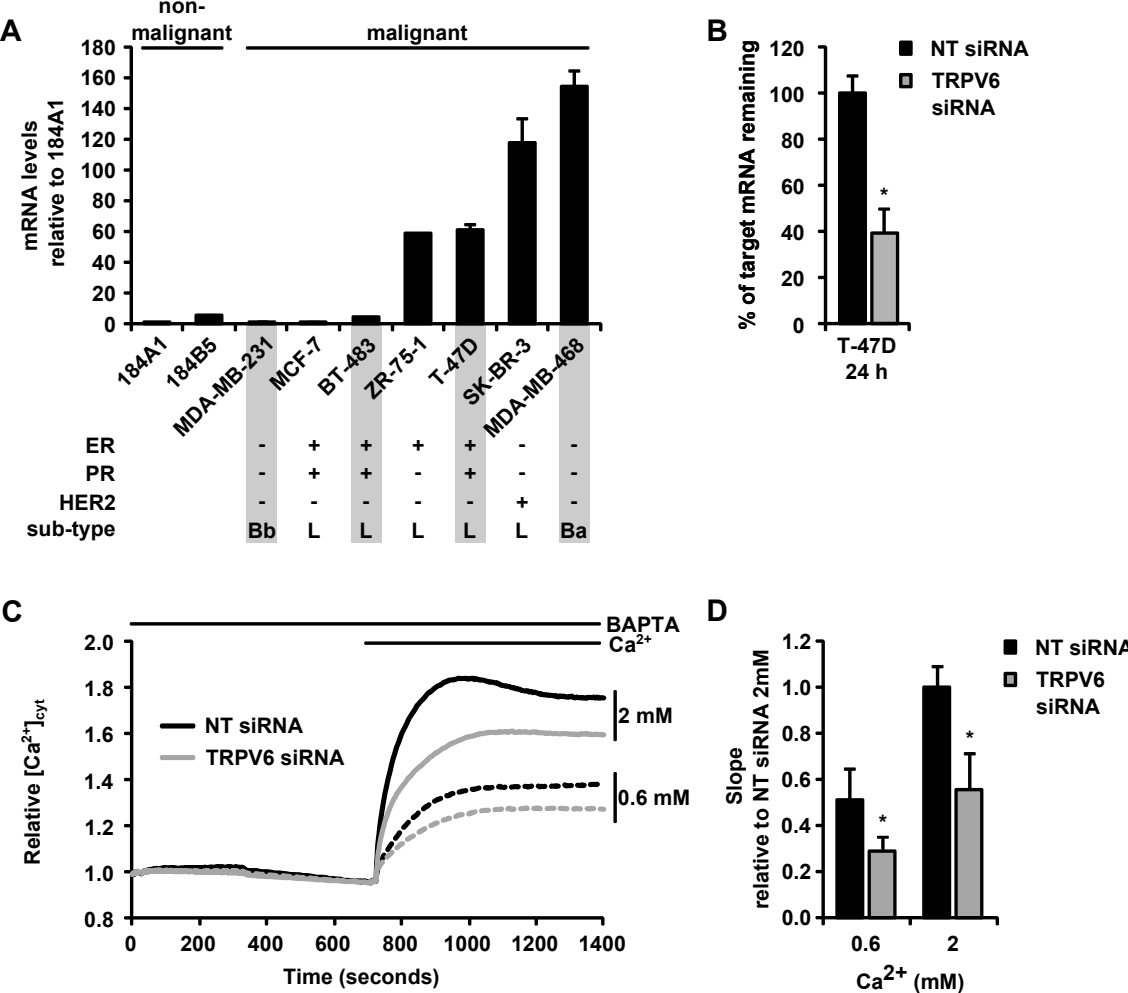
Figure 2: Effect of TRPV6 down-regulation in the T-47D breast cancer cell line. TRPV6 was knocked down in T-47D cells using siRNA, and the effect on viable cell number, cell cycle, and migration was assessed compared with non-targeting siRNA (NT-siRNA). A, Relative TRPV6 mRNA levels in T-47D breast cancer cells 120 h after treatment with non-targeting siRNA (NT siRNA) or TRPV6 siRNA. The data are mean \pm SD ($N = 3$) and are from three independent experiments.* $P < 0.05$ compared with NT siRNA using an unpaired t-test. B-F, Data are mean \pm SD ($N = 9$) from 3 independent experiments. * $P < 0.05$ compared with NT siRNA using an unpaired t-test. B, effect of TRPV6 knockdown on total cell number. C, effect of TRPV6 knockdown on the percentage of EdU positive cells. D and E, effect of TRPV6 down regulation on the cell cycle in T-47D cells that were treated with serum for 24 h (D) or 48 h (E) after serum deprivation.

The left panel depicts a representative frequency distribution of nuclear DAPI integrated intensity of three independent experiments. The right panel depicts the percentages of cells in G1, S and G2/M phase as mean \pm SD from three independent experiments performed in triplicate. * $P < 0.05$ compared with NT siRNA using an unpaired t-test. F, effect of TRPV6 siRNA on migration expressed as fluorescence relative to NT siRNA. * $P < 0.05$ compared with NT siRNA using an unpaired t-test.

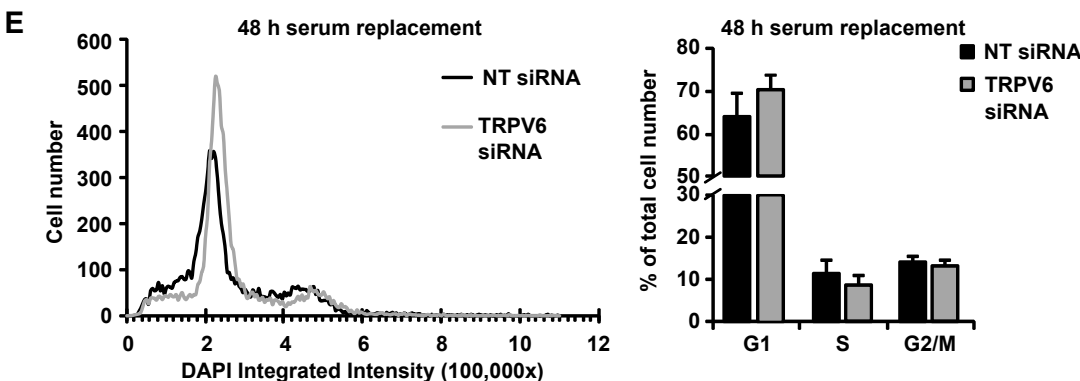
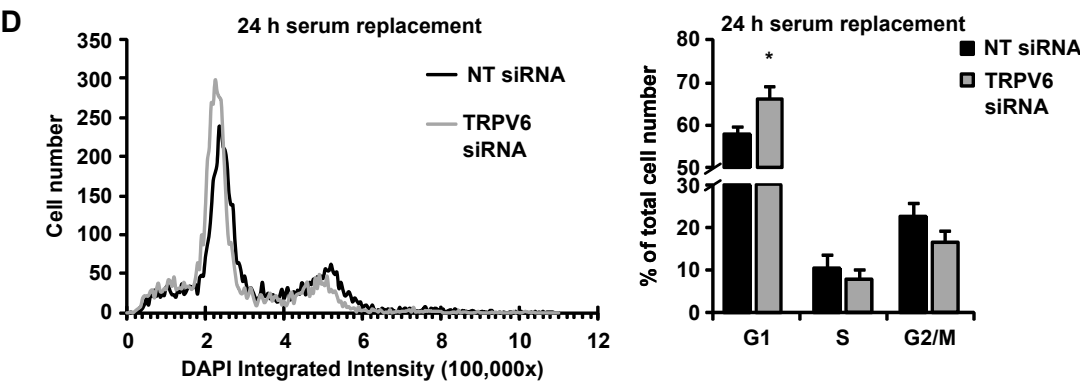
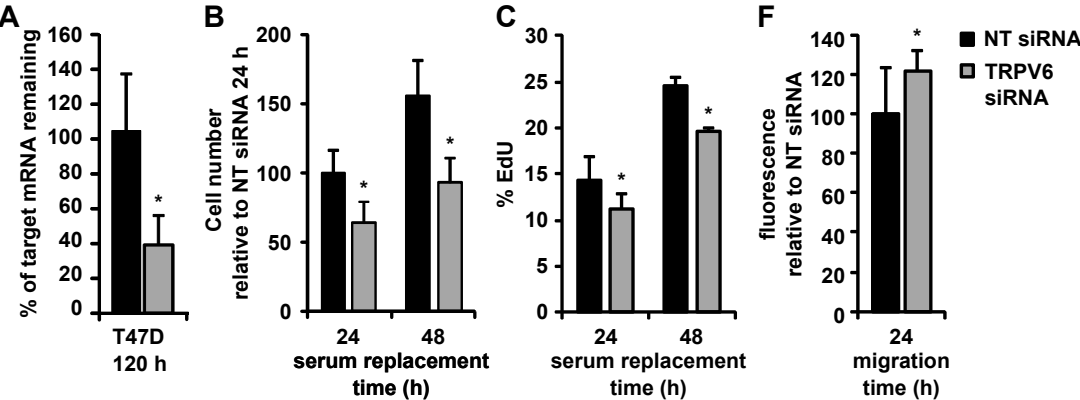
Figure 3: Characterization of TRPV6 copy number in breast cell lines. A, TRPV6 gene copy number in control genomic DNA (gDNA) and malignant MDA-MB-231, MCF-7, BT-483, ZR-75-1, T-47D, SK-BR-3 and MDA-MB-468 breast cancer cell lines. The data are mean \pm SD ($N = 8$) and are from two independent experiments carried out in quadruplicate. B, comparison of mRNA expression relative to 184A1 and gene copy number in breast cancer cell lines.

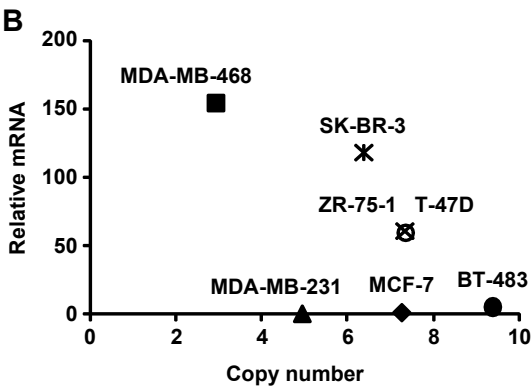
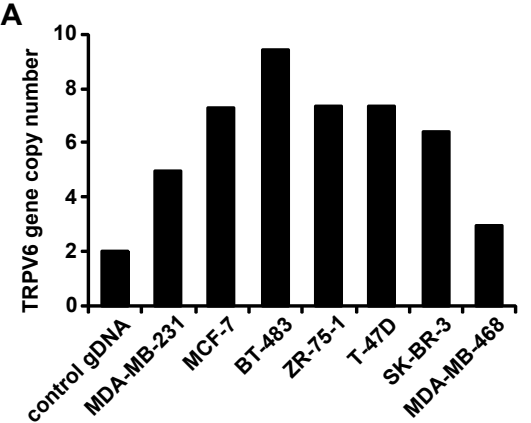
Figure 4: *TRPV6* gene copy number in breast tumors. A, chromosome 7 frequency plots of SNP-CGH data derived from samples of invasive breast tumors (from The Cancer Genome Atlas) classified as either HER2 or basal-like molecular subtype. X-axis: chromosome location (in base pairs); y-axis: proportion of cohort with gain along this chromosome. *TRPV6* gene region is highlighted by a red line. B, a profile of chromosome 7 copy number (from BAC aCGH) from an invasive ductal carcinoma. X-axis: chromosome location; y-axis: normalized, scaled log₂ ratios of individual BAC clones. The arrow indicates a specific amplification of the region harboring the *TRPV6* gene. C, correlation between *TRPV6* gene copy number and mRNA levels in the TCGA cohort of human breast tumors. Data were stratified according to molecular subtype. X-axis: DNA copy number at *TRPV6* gene region according to segmental DNA values (level 3 data); y-axis: log₂ lowess normalized values for TRPV6 mRNA expression levels. A Pearson's correlation coefficient (R-values) was calculated to measure the relationship between gene copy number and its mRNA expression profile.

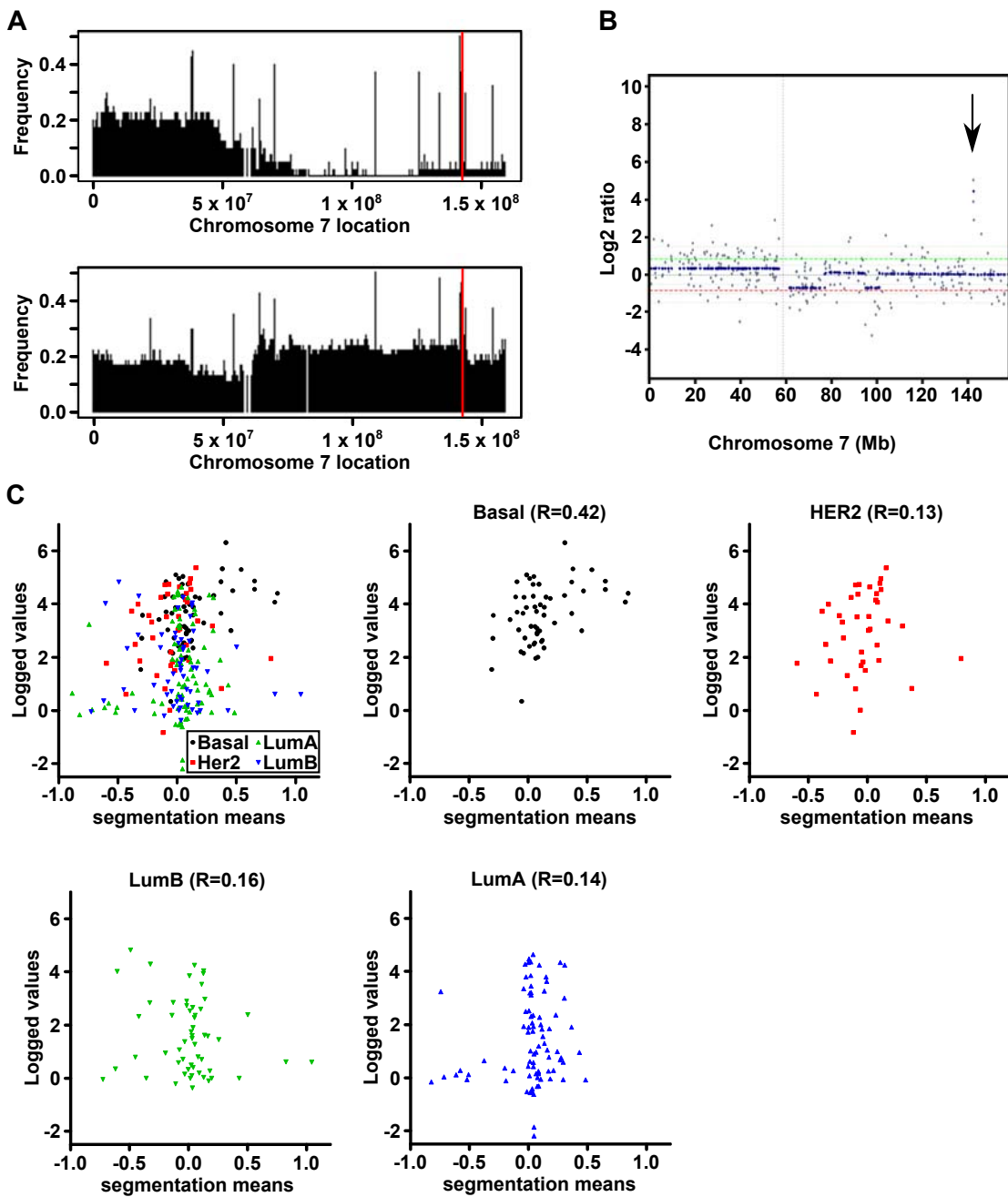
Figure 5: TRPV6 in breast cancer samples from two independent cohorts. Relative TRPV6 expression levels were assessed in the TCGA (A, C and E) and NKI-295 (B, D and F) microarray datasets. Horizontal lines represent median values and $*P < 0.05$ using Kruskal-Wallis test with Dunn's post-test for multiple comparisons. A and B, breast tumors were allocated to estrogen receptor (ER)-negative or ER-positive and * indicates significance compared to ER-positive. C and D, breast tumors were allocated to molecular subtypes and * and ^ indicates significance compared Luminal A and Luminal B, respectively. E, breast tumors were allocated to histopathological subtypes and immunophenotypes * indicates significance compared to ER-positive, HER2-negative; Duc, ductal; Lob, Lobular; Other, tumors of other histological type or with incomplete pathological/clinical data, e.g. no type or ER data. F, TRPV6 expression in the upper quartile is associated with reduced survival in breast cancer patients. Kaplan-Meier analysis, patient survival was compared between tumors in the upper, intermediate and lower quartile of TRPV6 expression. Significance was tested using the log-rank test.



Peters AA, Figure 1



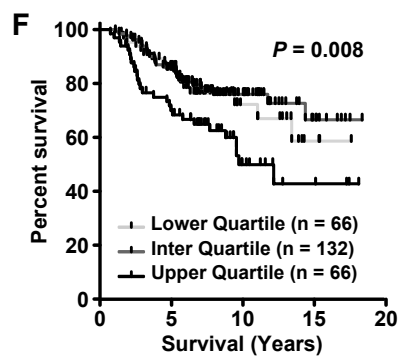
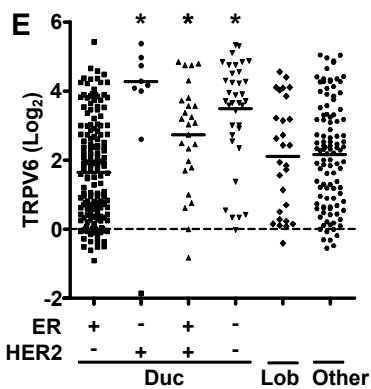
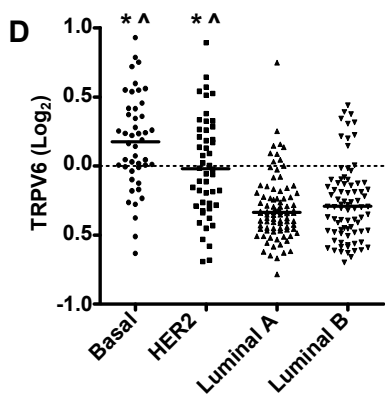
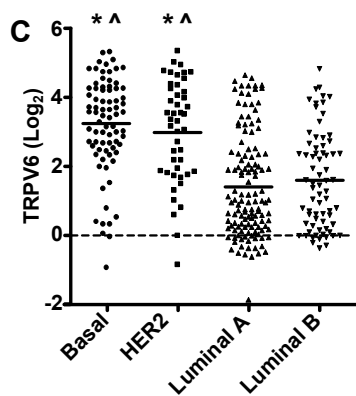
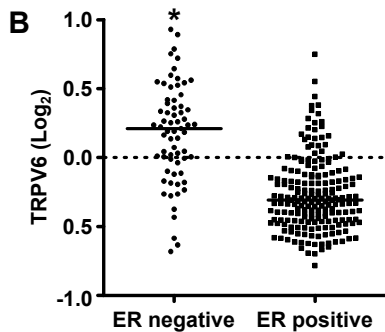
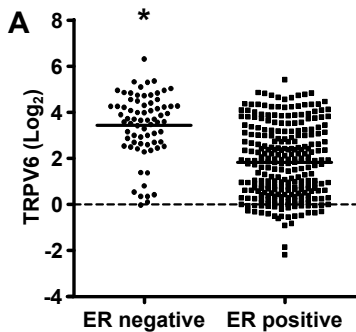




Peters AA, Figure 4

TCGA dataset

NKI295 dataset



Peters AA, Figure 5